Effect of pump-1 laser on Autler–Townes splitting in photoelectron spectrum of K_2 molecule*

Guo Wei(郭 玮)[a], Lu Xing-Qiang(路兴强)[b]†, Wang Xin-Lin(王新林)[a], and Yao Hong-Bin(姚洪斌)[c]

[a] School of Electric Engineering, University of South China, Hengyang 421001, China
[b] School of Nuclear Science and Technology, University of South China, Hengyang 421001, China
[c] Department of Basic Courses, Xinjiang Institute of Engineering, Urumqi 830091, China

(Received 30 July 2014; revised manuscript received 12 September 2014; published online 25 November 2014)

We theoretically investigate the Autler–Townes (AT) splitting in the photoelectron spectrum of four-level ladder K_2 molecule driven by a pump 1-pump 2-probe pulse via employing the time-dependent wave packet approach. The effects of the pump-1 laser intensity and wavelength on AT splitting are studied for the first time. The magnitude of AT splitting increases with increasing the pump-1 laser intensity. The triple splitting with asymmetric profile occurs due to the non-resonant excitation. The triple structure is transformed into a double structure (near-resonant region), and then becomes a peak (far-off resonant region) progressively as the pump-1 laser is detuned from the resonance wavelength, which can be explained in terms of the asymmetric excitation/population of dressed states. The splitting between adjacent peaks and the splitting between the two sideband peaks in the triplet do not change with the pump-1 pulse wavelength. The three peaks shift toward lower energy with the same shift $1/4^*\Delta_1$ as the pump-1 wavelength changes in near-resonant region. The asymptotic behaviors of AT splitting with the pump-1 laser intensity are interesting in the threshold points of the near-resonant region and the far-off resonant region.

Keywords: Autler–Townes splitting, photoelectron spectra, four-level ladder K_2 molecule

PACS: 33.60.+q, 33.20.Xx, 42.50.Hz **DOI:** 10.1088/1674-1056/24/1/013302

1. Introduction

The ac-Stark effect, also known as Autler–Townes (AT) splitting, occurs due to nonlinear interactions between light and matter in the presence of one or more strong variable radiation fields.[1] In recent years, the dependence of AT splitting on laser parameters, such as laser intensity,[2–27] laser wavelength,[4,5,8–11,16–21] pulse width,[6,7,22,24,25] pulse envelope,[27] and time delay[2,26,28,38] has been studied theoretically and experimentally in multi-level atomic/molecular systems of various configurations

For a three-level system, the AT double splitting generally can be observed by using a pump–probe laser configuration, and can be interpreted by the dressed-state theory. Wollenhaupt *et al.*[2,3] observed experimentally the AT double splitting in photoelectron spectra of K atoms, and studied the effects of pump intensity and time delay on AT doublet. They suggested that the asymmetry of the splitting is due to the non-resonant excitation, and the splitting monotonically increases with the laser intensity. Peng and Zheng[4,5] investigated single quantum dots driven simultaneously by pump–probe field in a three-level V-type system, and showed that the pump intensity and detuning affect the splitting, position and relative height of AT double peaks. Sun and Lou[6] obtained theoretically the AT double splitting in Na_2 molecules, and studied the effects of pump intensity and pulse width on the splitting. The longer pulse can induce the asymmetry of doublet. Yuan *et al.*[7] studied the effects of molecular rotation and alignment on the AT double splitting in Na_2. Liu *et al.*[8] indicated that probe wavelength and time delay have an effect on the AT double splitting and relative height in ladder Li_2 molecules. Yao and Zheng[9] and Yao *et al.*[1] observed the AT double splitting in K_2 molecules, and suggested that the pump intensity and wavelength determine the magnitude of splitting and the enhancement of peaks.

Nonlinear effects due to the quantum coherence effect have also been studied in four-level atomic systems of various configurations. The AT splitting in a four-level system shares some similar features with that in a three-level system. Wei *et al.*[11] and Han *et al.*[12] studied theoretically the ac Stark effect in a four-level V-type atomic system in the presence of three driving fields. It was found that the absorption spectra can have two or three peaks depending on the intensities and wavelengths of the driving fields. The intensity and wavelength of the second driving field have an effect on the AT splitting. They used the dressed state theory to explain the absorption peaks in the spectra. Many reports[13–16] studied the AT effect in a strongly driven electromagnetically induced transparency (EIT) resonance with a four-level Λ-type atomic system. It is found that the absorption spectrum has two or three peaks in general and their positions and relative intensi-

*Project supported by the National Natural Science Foundation of China (Grant Nos. 41104094 and 11174119), the Research Fund for the Doctoral Program of Higher Education of China (Grant No. 20114324120002), the Research Foundation of Education Bureau of Hunan Province, China (Grant No. 12C0370), and the Scientific Research Foundation for the Returned Overseas Chinese Scholars.

†Corresponding author. E-mail: luxingqiang@163.com

© 2015 Chinese Physical Society and IOP Publishing Ltd

ties are strongly affected by the intensities of the driving fields and their detunings. Echaniz *et al.*[17] and Wang and Zheng[18] expected a three-peak absorption spectrum in a four-state N-type atomic system, and studied the trajectories of three peaks as a function of Rabi frequency and detuning of one couple field. The expectation is verified in the Rb sample. Dutta and Mahapatra[19] expected a two or three-peak emission spectrum in a four-state N-type atomic system, and suggested that the double splitting increases as the intensity of one couple field augments. Sandhya[20] studied the absorption profile of a four-level ladder atomic system interacting with three driving fields. It is expected that there is three-peak absorption (dynamic splitting) with strong middle transition coupling. The three-peak splitting is also observed in the absorption profile of a photonic crystal doped with five-level nanoparticles, and the features of triple splitting with different intensities and those of detuning are also studied.[21]

For a four-level ladder system, Meier and Engel,[22] and Meier *et al.*[23] observed the AT triple splitting in Na_2 molecules driven by three driving fields, and studied the effect of pulse width on the AT splitting. Longer pulse indicates asymmetric AT triplet. Hu *et al.*[24,25] observed the AT triple splitting in Li_2 molecules driven by three driving fields, and studied the effect of pulse width on the splitting. A longer pulse indicates asymmetric AT triple splitting. Liu *et al.*[26] indicated that the probe intensity and time delay affect the peak height of AT splitting of Li_2 molecules using a cw–pump–probe field. Yao and Zheng[27] observed the AT triple splitting with asymmetric profiles in four-level K_2 molecules driven by three driving fields in the near-resonant region, and studied the effects of intensity, wavelength, and envelope on AT splitting when the parameters of the three laser fields change simultaneously, but they did not study the phenomenon in the resonant and far-off resonant region nor the effect of the parameters of some pump laser field on the AT splitting.

Most of the above experimental and theoretical studies on the dependence of AT splitting on laser intensity and wavelength are involved with the four-level N, V, and Λ configuration. Few studies relate to the ladder configuration. No study has focused on the effects of the intensity and wavelength of the first pump pulse on AT splitting in a four-level ladder K_2 molecule. In this paper, we investigate the natures of the AT splittings in the photoelectron spectra of the four-level ladder K_2 molecule driven by pump-1, pump-2, and probe pulses by the time-dependent quantum wave packet method. We discuss the effects of the pump-1 laser intensity and wavelength on AT splitting for three cases: resonant pulse, near resonant pulse, and far-off resonant pulse. The corresponding features are different at different intensities and wavelengths of the pump-1 pulses.

2. Formalism

In this paper, we model a four-level ladder K_2 molecule by four electronic states, ground state $|X\rangle\,{}^1\Sigma_g^+$, two excited states $|A\rangle\,{}^1\Sigma_u^+$ and $|2\rangle\,{}^1\Pi_g^+$, and ionic ground state $|X^+\rangle\,{}^2\Sigma_g^+$; for simplicity, they are abbreviated to $|X\rangle$, $|A\rangle$, $|2\rangle$, and $|X^+\rangle$ in order. Figure 1 shows the potential energy curves of K_2 in this work. A similar model to the model of the K_2 molecule is also employed in experimental[29,30] and theoretical studies.[27,31] In our treatment, we consider the case that pump-1, pump-2, and probe laser fields are simultaneously applied to the K_2 molecule. The molecule in the ground state $|X\rangle$ is resonantly excited to the excited state $|A\rangle$ by the pump-1 laser pulse with the central wavelength $\lambda_1 = 848$ nm. The pump-2 laser pulse with the central wavelength $\lambda_2 = 785$ nm then resonantly excites the molecule from $|A\rangle$ to $|2\rangle$. Finally, the probe laser pulse with the central wavelength $\lambda_3 = 785$ nm is used to detect the emitted photoelectron from the ionization state $|X^+\rangle$. We neglect the rotational degree of freedom in our treatment, since the rotational motion of the heavy K_2 molecule is almost frozen on a femtosecond time scale.

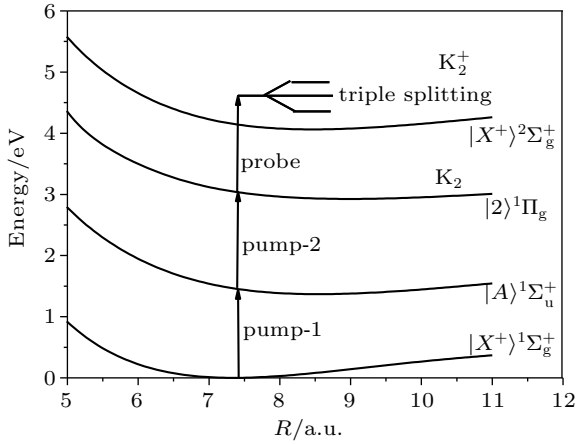


Fig. 1. Potential energy curves of the K_2 molecule used in this work. The arrows indicate the excitation energies of 1.462 eV (848 nm), 1.579 eV (785 nm), and 1.579 eV (785 nm) respectively.

Under the Born–Oppenheimer approximation, the wavefunction Ψ can be obtained by solving the time-dependent Schrodinger equation

$$i\hbar\frac{\partial}{\partial t}\Psi = H\Psi. \tag{1}$$

The Hamiltonian H of the system can be written as

$$H = H_S + H' = T + V + H', \tag{2}$$

where $H_S = T + V$ is the Hamiltonian of the K_2 molecule, T is the operator of the kinetic energy of the nucleus, V is the potential energy of the system, and H' is the interaction between the K_2 molecule and the laser field. For the four-state model, the wave functions can be written in the form of column vector

$$\Psi = (\psi_X, \psi_A, \psi_2, \psi_{ion})^T, \tag{3}$$

where ψ_X, ψ_A, ψ_2, and $\psi_{\rm ion}$ are the wave functions for the ground state $|X\rangle$, excited states $|A\rangle$ and $|2\rangle$, and ionization state $|X^+\rangle$, respectively. The ionization state is a continuum state, and it is discretized into a band of quasicontinuum states in terms of the energies of the emitted photoelectron for the numerical calculations. The ionization state $\psi_{\rm ion}$ can be further expressed as

$$\psi_{\rm ion} = \left(\psi^{(1)}, \psi^{(2)}, ..., \psi^{(N)}\right)^{\rm T}, \tag{4}$$

where N is the number of discrete states of the K_2 ion.

The kinetic energy T can be expressed as

$$T = -\frac{\hbar^2}{2\mu}\frac{\partial^2}{\partial R^2}\mathscr{T}, \tag{5}$$

where μ is the reduced mass of the nuclei, R is the distance between the nuclei in the K_2 molecule,

$$\mathscr{T} = \begin{pmatrix} 1 & 0 & 0 & \mathfrak{o} \\ 0 & 1 & 0 & \mathfrak{o} \\ 0 & 0 & 1 & \mathfrak{o} \\ \tilde{\mathfrak{o}} & \tilde{\mathfrak{o}} & \tilde{\mathfrak{o}} & \mathbb{I} \end{pmatrix},$$

and $\mathfrak{o} = (0,0,\ldots,0)$ is a zero vector with N-component, $\tilde{\mathfrak{o}}$ is the transverse of the vector $\mathfrak{o}$, and $\mathbb{I}$ is an $N \times N$ unit matrix.

The potential V can be expressed as

$$V = \begin{pmatrix} V_X & 0 & 0 & \mathfrak{o} \\ 0 & V_A & 0 & \mathfrak{o} \\ 0 & 0 & V_2 & \mathfrak{o} \\ \tilde{\mathfrak{o}} & \tilde{\mathfrak{o}} & \tilde{\mathfrak{o}} & \mathbb{V} \end{pmatrix}, \tag{6}$$

where V_X, V_A, and V_2 are the potential curves of the ground state $|X\rangle$ excited states $|A\rangle$ and $|2\rangle$, respectively. $\mathbb{V}$ is an $N \times N$ matrix, which is the discretized states of ionization state $|X^+\rangle$. It can be written as

$$\mathbb{V} = V_X + \mathbb{I} + \begin{pmatrix} \xi^{(1)} & 0 & \cdots & 0 \\ 0 & \xi^{(2)} & \cdots & 0 \\ \vdots & \vdots & \ddots & \vdots \\ 0 & 0 & 0 & \xi^{(N)} \end{pmatrix}, \tag{7}$$

where $\xi^{(i)} = (i-1)\Delta\xi \quad (i = 1,2,\ldots N)$ is the energy of the emitted photoelectron.

The interaction H' between K_2 molecule and laser field is given by

$$H' = \begin{pmatrix} 0 & W_{XA} & 0 & o \\ W_{XA} & 0 & W_{A2} & o \\ 0 & W_{XA} & 0 & \mathbb{W}_{2i} \\ \tilde{\mathfrak{o}} & \tilde{o} & \tilde{\mathbb{W}}_{2i} & \mathbb{O} \end{pmatrix}, \tag{8}$$

where $\tilde{\mathbb{W}}_{2i} = \left(W_{2i}^{(1)}, W_{2i}^{(2)}, \ldots, W_{2i}^{(N)}\right)$ is the vector of coupling between $|2\rangle$ and $|X^+\rangle$ states via the laser field with the N-component, and $\mathbb{O}$ is the $N \times N$ zero matrix. The coupling between two states via an external laser field is given by

$$W_{XA} = \hbar R_1(R)\cos(\omega_1 t),$$
$$W_{A2} = \hbar R_2(R)\cos(\omega_2 t),$$
$$W_{2i} = \hbar R_3(R)\cos(\omega_3 t),$$

where $R_1 = \frac{1}{\hbar}\mu_{XA}(R)\,e_1 f(t)$, $R_2 = \frac{1}{\hbar}\mu_{A2}(R)\,e_2 f(t)$, and $R_3 = \frac{1}{\hbar}\mu_{2i}(R)\,e_3 f(t)$ are the Rabi frequencies of laser fields for $|X\rangle \to |A\rangle$ state, $|A\rangle \to |2\rangle$ state, and $|2\rangle \to |X^+\rangle$ state, respectively; $\mu_{XA}(R)$, $\mu_{A2}(R)$, and $\mu_{2i}(R)$ are the transition dipole moments between different electronic states; e_1, e_2, and e_3 are the amplitudes of laser fields; ω_1, ω_2, and ω_3 are angular frequencies; and $f(t)$ is the envelope which we choose to be a Gaussian function $f(t) = \exp\left[-4\ln 2\,(t/\tau)^2\right]$, with τ being the full width at half maximum (FWHM) of the pulse, which is 30 fs in our numerical calculations.

The photoelectron spectrum as a function of the electronic energy $\xi^{(i)}$, can be obtained as[22–27]

$$P\left(\xi^{(i)}\right) = \lim_{t\to\infty}\int {\rm d}R\left|\psi^{(i)}\left(R,t,\xi^{(i)}\right)\right|^2. \tag{9}$$

The potential energy curves of the K_2 molecule employed in our calculations are cited from Refs. [32]–[35]. These potential curves are in good consistence with relevant spectroscopic constants of experimental results[36–38] and the detailed information about the potentials can be obtained from Ref. [39]. The transition dipole moments are cited from Ref. [40]. In this paper, the energies of the emitted photoelectron $\xi^{(i)}$ span over 0–2 eV, and the number of discrete states of K_2 ions, N, equals 120. The time-dependent Schrodinger equation (1) is solved by the "split-operator Fourier" method exactly.[41–44] The K_2 molecule is initially populated on its vibrational ground state of the $|X\rangle$ state.

3. Results and discussion

We consider the effect of pump-1 laser intensity on the photoelectron spectrum in the resonant region. Figure 2 shows the photoelectron spectra each as a function of pump-1 laser intensity I_1 at $I_2 = I_3 = 4I_0$ ($I_0 = 1.0 \times 10^{11}$ W/cm^2), $\lambda_1 =$ 848 nm, and $\lambda_2 = \lambda_3 = 785$ nm. The peaks of photoelectron spectra show the triple splitting with symmetric profiles: one central and two sideband peaks at $I_1 \geq 2I_0$, and no splitting at $I_1 \leq 2I_0$. The triple splitting with asymmetric profiles of the K_2 molecule has been obtained in the near resonant region of the pump-1 pulse with $\lambda_1 = \lambda_2 = \lambda_3 = 785$ nm. However, the resonant case was not studied.[27] The triplet with symmetric profiles has been observed in four-level ladder Na_2 molecule[22,23] and Li_2 molecule,[24,25] and it is similar to the expected three-peak absorptions (dynamic splittings) in four-level atomic systems with various configurations interacting with three driving fields,[11,12,14,15,17,18,20] which can be explained in terms of

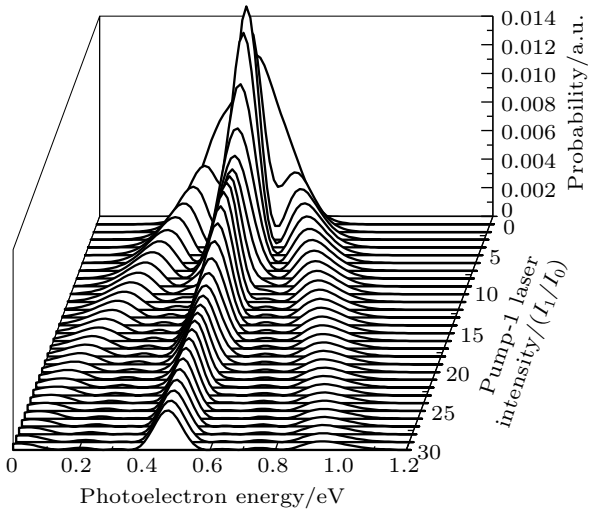


Fig. 2. Photoelectron spectra for various laser intensities of pump-1 filed. The parameters are as follows: $I = 1.0 \times 10^{11}$ W/cm^2, $I_2 = I_3 = 4I_0$, $\lambda_1 = 848$ nm, $\lambda_2 = \lambda_3 = 785$ nm, and $\tau = 30$ fs.

the dressed state formalism. It is also observed in the absorption profiles in a photonic crystal doped with five-level nanoparticles.[21] The splitting pattern of photoelectron spectrum is so-called AT splitting. According to the explanation of ac-Stark splitting in dressed state picture, the three-peak structure arises from the sufficient Rabi oscillation in the resonant region in the ionization process.[22–27] From the dressed state theory, the excited state $|2\rangle$ is dressed by the laser field and splits into three substrates $|\alpha\rangle$, $|\beta\rangle$, and $|\gamma\rangle$, which correspond to the three peaks from left to right in the photoelectron spectrum respectively. Here, we assume that the energy of the $|\gamma\rangle$ state is higher than that of the $|\beta\rangle$ state, which in turn is higher than that of the $|\alpha\rangle$ state. Another important feature in Fig. 2 is that the magnitude of the triple splitting increases with the increasing laser intensities of the pump-1 pulse. This is similar to the observations in three-level K,[2,3] Rb,[45] K_2,[9,10] and Na_2,[4] and four-level K_2.[21] A similar feature is shown in the absorption spectrum for a four-level atomic system interacting with three driving fields.[11–20,46,47] Figure 3 shows the peak positions for the spectra shown in Fig. 2 as a function of pump-1 laser intensity I_1 (Fig. 3(a)) and pump-1 Rabi frequency R_1 (Fig. 3(b)), respectively. The position of the central peak is around 0.474 eV, which simply is $E_{v0} + \sum \hbar\omega_k - V_I(R_0)$,[6,22,24] with E_{v0} being the energy of the vibrational ground state, $\hbar\omega_k$ the photon energy, and $V_I(R_0)$ the potential of the $|X^+\rangle$ state at equilibrium distance R_0 of the neutral ground state, which are indicated with arrows in Fig. 1. These three peaks are at $0.474 - R/2$, 0.474, and $0.474 + R/2$ (effective Rabi frequency $R = \sqrt{R_1^2 + R_2^2}$[12,14,17,22–27,48]), which correspond to three substates respectively, and are plotted as a solid line in Fig. 3(b), showing that they are in good agreement with the numerical results. It is easy to know the asymptotic behaviors for $R_1 \ll R_2$ and $R_1 \gg R_2$ respectively. When the pump-1 field is weak ($R_1 \ll R_2$), there is a linear splitting proportional to $R_2/2$. On the other hand, with a very large R_1 ($R_1 \gg R_2$), the two side peaks approach a linear splitting proportional to $R_1/2$. These are plotted as dashed straight lines and dotted straight lines in Fig. 3(b). From Fig. 2, it is noted that as the pump-1 laser intensity increases, more higher-order peaks start to emerge. The spectrum consists of pairs of peaks. The emergence of more peaks with increasing laser intensity has been observed before in three-level Λ-type and ladder atoms[49–52] in the on-resonant and out-resonant cases. In the paper, we focus on the three main peaks in the photoelectron spectra.

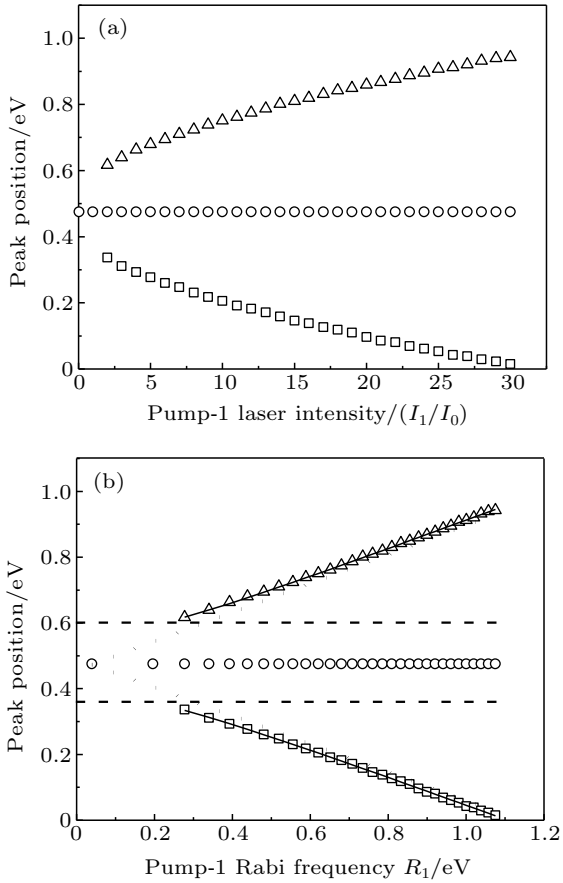


Fig. 3. Peak positions for the spectra in Fig. 2 as a function of (a) pump-1 laser intensity I_1 and (b) pump-1 Rabi frequency R_1. Also shown is the result using the dressed-state formalism (curves in solid lines). The dashed straight lines and dotted straight lines indicate the asymptotic behaviors for $R_1 \ll R_2$ and $R_1 \gg R_2$, respectively. All the other parameters are the same as those in Fig. 2.

We also pay attention to the effects of the pump-1 wavelength on the photoelectron spectrum. Figure 4 demonstrates the photoelectron spectra for different wavelengths of pump-1 (648–1188 nm) while keeping the pump-2 resonant, i.e. $\lambda_2 = 785$ nm, at $I_1 = I_2 = I_3 = 4I_0$. The pump-1 field detuning is given by $\Delta_1 = \omega_1 - \omega_{AX}$, where ω_{AX} is the frequency of the $|X\rangle \rightarrow |A\rangle$ state. From Fig. 4 it is noted that the spectrum exhibits a triple splitting with symmetric profiles when the pump-1 field has a zero detuning (i.e., $\lambda_1 = 848$ nm), while asymmetric profiles arise as the pump-1 field is moved off resonance 848 nm. The asymmetry of the splitting is

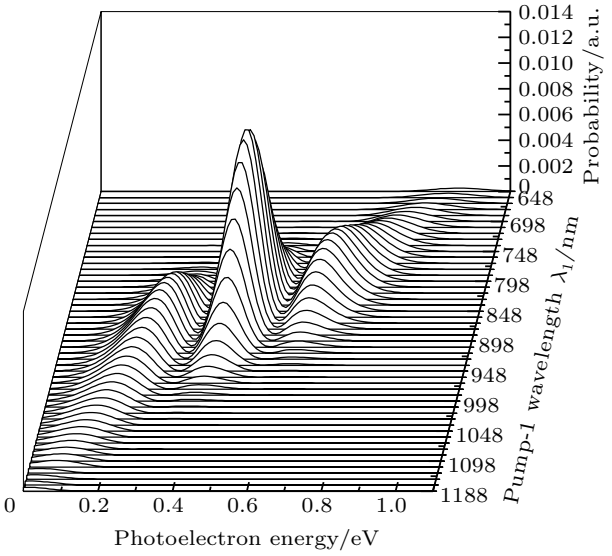


Fig. 4. Photoelectron spectra for various pump-1 laser wavelengths (648 nm–1188 nm) with pump-2 resonant. The parameters are as follows: $I = 1.0 \times 10^{11}$ W/cm^2, $I_1 = I_2 = I_3 = 4I_0$, $\lambda_2 = \lambda_3 = 785$ nm, and $\tau = 30$ fs.

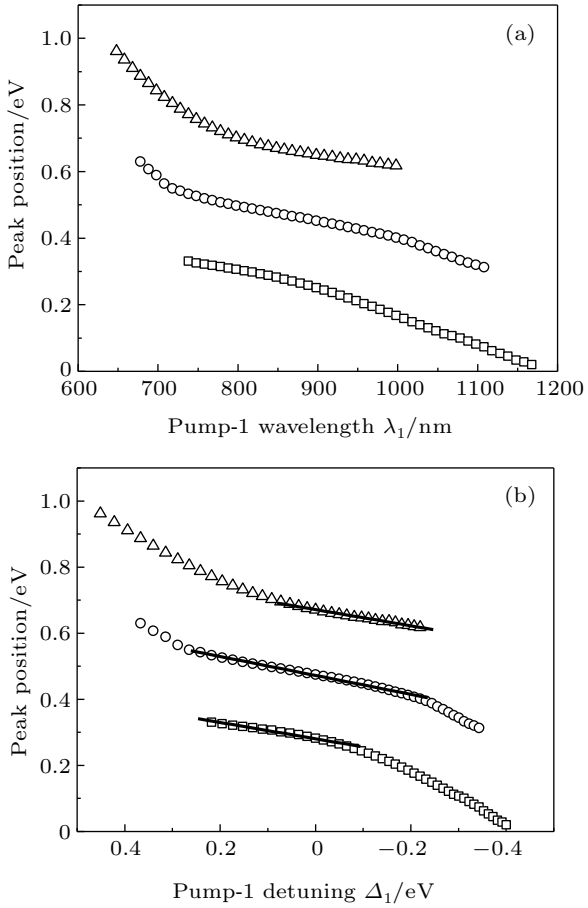


Fig. 5. Peak positions for the spectra in Fig. 4 versus (a) pump-1 laser wavelength λ_1 and (b) pump-1 detuning Δ_1. Other parameters are the same as those in Fig. 4.

due to the nonresonant excitation. The triple splitting with asymmetric profiles of four-level K_2 molecule in the near resonant region of pump-1 with $\lambda_1 = \lambda_2 = \lambda_3 = 785$ nm has been observed by Yao and Zheng.[27] This asymmetry has been observed in double splitting in three-level K atoms[2] and K_2 molecules[9] and other atoms.[5,52–54] A similar feature is shown in the three-peak absorption profiles[47,55] or emission spectra[19] in a four-level atomic system and in five-level atoms.[21] The three peaks shift toward the lower energy with increasing pump-1 wavelength. This is because the longer wavelength indicates the lower photon energy, resulting in lower photoelectron energy. This energy shift trend with the laser wavelength is qualitatively identical with the observation in three/four-level atoms/molecules.[2,5,11,27,46,54] This is also identical with the observation in a four-level K_2 molecule with a secant pulse and a square pulse by Yao and Zheng, but they did not give the results with a Gaussian pulse.[27] Figure 5 shows the peak positions for the spectra shown in Fig. 4 as a function of pump-1 wavelength λ_1 (Fig. 5(a)) and pump-1 detuning Δ_1 (Fig. 5(b)), respectively. The linear fits are $0.281 + 0.246\Delta_1$, $0.474 + 0.267\Delta_1$, and $0.671 + 0.245\Delta_1$, for three peaks from left to right in the photoelectron spectrum, respectively in the near resonant region. This indicates that both peaks shift $1/4^*\Delta_1$ in the region. This peak shift behavior is not shown in earlier work in the four-level ladder system, but in other configurations. Sadeghi *et al.*[13] studied the AT effect in a strongly electromagnetically induced transparency (EIT) resonance with a four-level Λ-type atomic system, and suggested that the splitting between adjacent peaks in the triplet of the absorption spectrum may be equal or unequal, depending on different detunings of two driving fields. Echaniz *et al.*[17] and Wang and Zheng[18] studied the trajectories of three peaks as a function of detuning of the second couple field with the four-level N-type Rb system, and suggested that the peak shift is not linear with respect to the detuning, and the splitting between adjacent peaks in the triplet is unequal to that in the resonant case. In contrast to these suggestions in the detuning case of the driving field, comparing Fig. 5 with Fig. 3, we can see that neither the splitting (0.185 eV) between adjacent peaks nor the splitting (0.370 eV) between the two sideband peaks in the triplet changes with the pump-1 pulse wavelength. In Figs. 4 and 5, an important and interesting feature is that the triple structure is transformed into a double structure and then become one peak progressively as pump-1 is detuned from the resonance wavelength 848 nm. The threshold points are $\Delta_1 = \pm 0.24$ eV (i.e., $\lambda_1 = 728$ nm or 1008 nm) and $\Delta_1 = \pm 0.34$ eV (i.e., $\lambda_1 = 668$ nm or 1118 nm) for three-to-two transformation and two-to-one transformation, respectively. The peak disappearance can be explained by the asymmetric excitation/population of dressed states. For the resonant case (i.e., $\lambda_1 = 848$ nm), the dressed states $|\alpha\rangle$ and $|\gamma\rangle$ will be equally excited because of their symmetries, so the two symmetric side peaks are observed. However, if the pump-1 wavelength scans from 728 nm to 1008 nm, the dressed states $|\alpha\rangle$ and $|\gamma\rangle$ will be shifted and excited differently, and the two asymmetric side peaks are obtained at near resonant pump-1

pulse. For example, as the pump-1 wavelength increases from resonance, the longer wavelength indicates the lower photon energy, the dress state $|\alpha\rangle$ will be excited/populated more easily than substate $|\gamma\rangle$, resulting in the enhancement of the left side peak over the right side peak. The disappearance of the right/left side peak for $\lambda_1 \geq 1008$ nm/$\lambda_1 \leq 728$ nm indicates that the population on the $|\gamma\rangle$ / $|\alpha\rangle$ substate is zero. The central peak and right/left side peak disappear for $\lambda_1 \geq 1118$ nm/$\lambda_1 \leq 668$ nm in the far-off resonant pump-1 pulse. This indicates that only the substate $|\alpha\rangle$ is populated in the far-off resonant pump-1 pulse region.

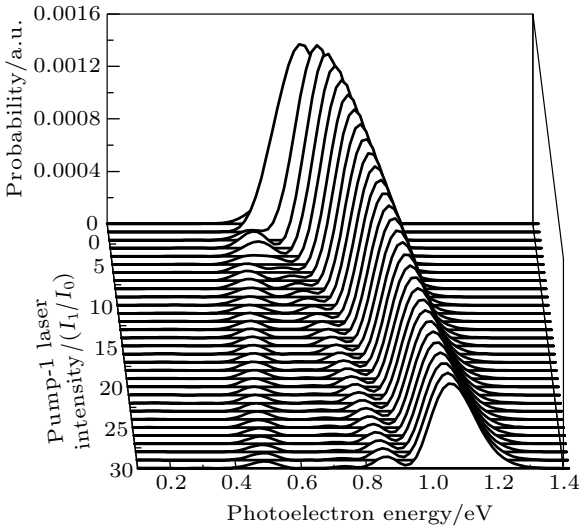


Fig. 6. Photoelectron spectra for various pump-1 laser intensities at the first threshold point. The parameters are as follows: $I = 1.0 \times 10^{11}$ W/cm^2, $I_2 = I_3 = 4I_0$, $\lambda_1 = 728$ nm, $\lambda_2 = \lambda_3 = 785$ nm, and $\tau = 30$ fs.

We consider the effect of pump-1 laser intensity on the photoelectron spectrum in the threshold region (the transformation of three peaks to two peaks), i.e. $\lambda_1 = 728$ nm. The result is shown in Fig. 6. A comparison of Fig. 6 with Fig. 2 shows that in Fig. 6, the left side peak disappears and only the central peak and right side peak are in the photoelectron spectrum. These two peaks are at 0.495, $0.495+R'/2$ (effective Rabi frequency $R' = \sqrt{R_1^2 + R_2^2 + \Delta_1^2}$[45,53]). The position of the right side peak changes, while the position of the central peak does not change as the pump-1 laser intensity increases. One peak neighbouring the right side peak emerges for $I_1 \geq 6I_0$, the same as that in the resonant case (see Fig. 2). The emergence of more peaks with increasing the laser intensity in the out-resonant case has been observed in a three-level atom system.[49,52] The peak positions of these two main components (central and right side peaks) are plotted in Fig. 7 as a function of I_1 (Fig. 7(a)) and R_1 (Fig. 7(b)), respectively, and are again consistent with the prediction of the dressed-state formalism (solid lines in Fig. 7(b)). It is easy to know the asymptotic behaviors for $R_1 \ll R_2$ and $R_1 \gg R_2$, respectively. When the pump-1 field is weak ($R_1 \ll R_2$), there is a linear splitting proportional to $\sqrt{R_2^2 + \Delta_1^2}/2$. The right side peak approaches to a linear splitting proportional to $R_1/2$ as the pump-1 field is strong ($R_1 \gg R_2$). These are plotted as dashed straight lines and dotted straight lines in Fig. 7(b).

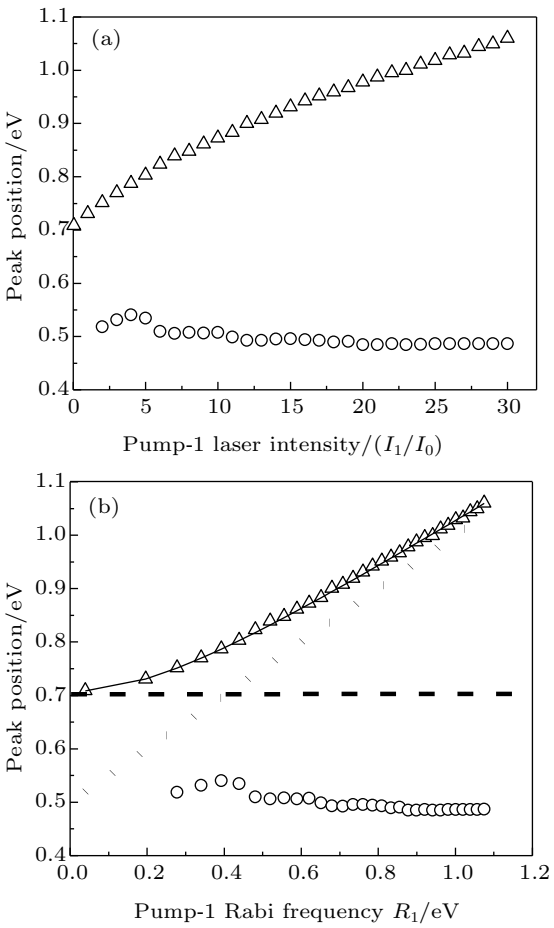


Fig. 7. Peak positions for the spectra in Fig. 6 versus (a) pump-1 laser intensity I_1 and (b) pump-1 Rabi frequency R_1. Also shown is the result using the dressed-state formalism (curve shown by solid line). The dashed straight lines and dotted straight lines indicate the asymptotic behaviors for $R_1 \ll R_2$ and $R_1 \gg R_2$. All the other parameters are the same as those in Fig. 6.

We also consider the effect of pump-1 laser intensity on the photoelectron spectrum in another threshold region (the transformation of two peaks to one peak), i.e. $\lambda_1 = 668$ nm. The result is shown in Fig. 8. A comparison of Fig. 8 with Figs. 2 and 6 shows that the central peak and left side peak disappear, only a right side peak exists in the photoelectron spectrum. The position of the right side peak peak is $0.595 + R'/2$ (effective Rabi frequency $R' = \sqrt{R_1^2 + R_2^2 + \Delta_1^2}$[45,53]). One peak neighbouring the right side peak emerges for $I_1 \geq 6I_0$, the same as that in the resonant case and near-resonant case (see Figs. 2 and 6). The peak position of one main component (right side peak) is plotted as a function of I_1 (Fig. 9(a)) and R_1 (Fig. 9(b)), respectively, and the result is in agreement with the prediction of the dressed-state formalism (solid line in Fig. 9(b)). The asymptotic behavior is the same as that in

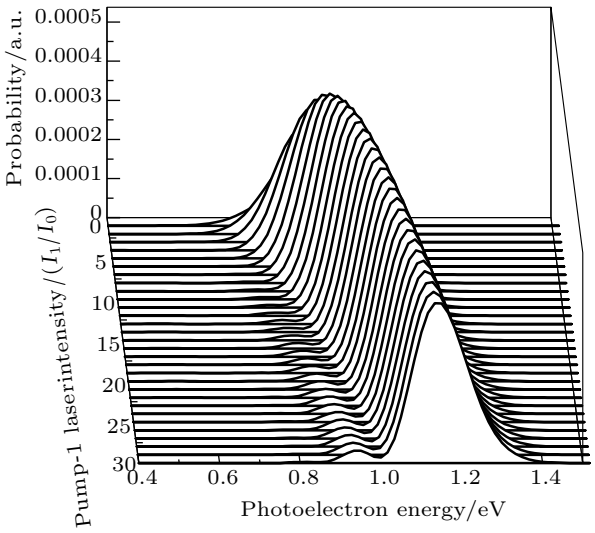


Fig. 8. Photoelectron spectra for various pump-1 laser intensities at the second threshold point. The parameters are as follows: $I_0 = 1.0 \times 10^{11}$ W/cm^2, $I_2 = I_3 = 4I_0$, $\lambda_1 = 668$ nm, $\lambda_2 = \lambda_3 = 785$ nm, and $\tau = 30$ fs.

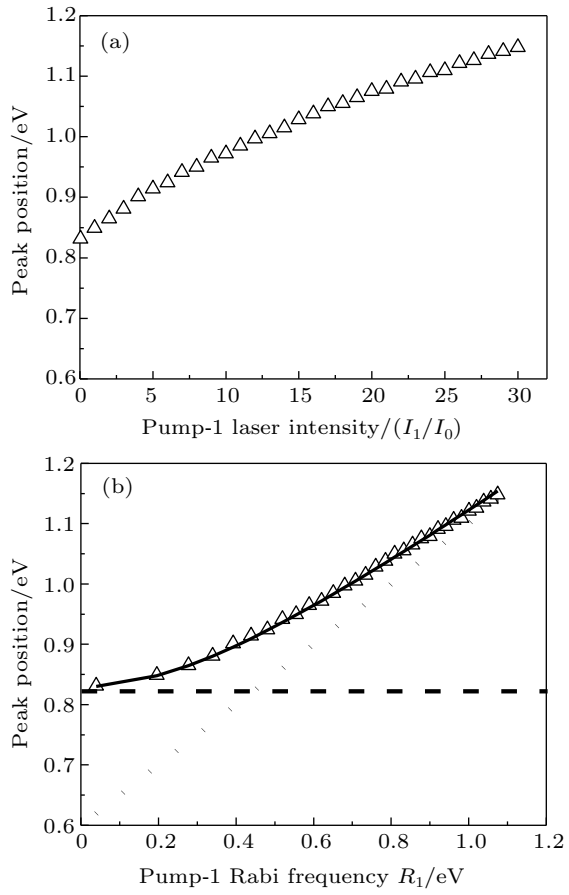


Fig. 9. Peak positions for the spectra in Fig. 8 versus (a) pump-1 laser intensity I_1 and (b) pump-1 Rabi frequency R_1. Also shown is the result using the dressed-state formalism (curve shown by the solid line). The dashed straight lines and dotted straight lines indicate the asymptotic behaviors for $R_1 \ll R_2$ and $R_1 \gg R_2$. All the other parameters are the same as those in Fig. 8.

the near-resonant case for $R_1 \ll R_2$ and $R_1 \gg R_2$, respectively. There is a linear splitting proportional to $\sqrt{R_2^2 + \Delta_1^2}/2$ for the weak pump-1 field ($R_1 \ll R_2$), while the right side peak approaches a linear splitting proportional to $R_1/2$ for the strong pump-1 field ($R_1 \gg R_2$). These are plotted as a dashed straight line and a dotted straight line in Fig. 9(b).

4. Conclusions

In this paper, we theoretically investigate the nature of AT splitting in the photoelectron spectrum of the four-level ladder K_2 molecule by employing the time-dependent wave packet approach. The observation of the photoelectron spectrum maps the information on the dressed state. The effects of the pump-1 laser intensity and wavelength on AT splitting are studied in detail for the first time for three cases: resonant pulse, near resonant pulse, and far-off resonant pulse.

In the resonant region, for fixed intensities of pump-2 and probe fields, the photoelectron spectra show the triple splitting with symmetric profiles (in peak height and splitting of two adjacent peaks), and the AT splitting increases with increasing pump-1 intensity. When the pump-1 field is weak ($R_1 \ll R_2$), there is a linear splitting proportional to $R_2/2$. On the other hand, with a very large R_1 ($R_1 \gg R_2$), the two side peaks approach a linear splitting proportional to $R_1/2$.

In the nonresonant region, for the fixed intensities of three fields, the photoelectron spectra show that neither the triple splitting with asymmetric profiles (in peak height), nor the splitting (0.185 eV) between adjacent peaks, nor the splitting (0.370 eV) between two sideband peaks in the triplet changes with the pump-1 pulse wavelength. The three peaks shift toward lower energy with the same shift $1/4^*\Delta_1$ as the pump-1 wavelength changes in the near resonant region (i.e., 738 nm $\leq \lambda_1 \leq$ 998 nm). As pump-1 is detuned from the resonance wavelength 848 nm, the triple structure is transformed into a double structure (near-resonant region), and then becomes a peak (far-off resonant region) progressively. This can be explained by the asymmetric excitation/population of dressed states.

At the two threshold points of the transformation (three peaks to two peaks and two peaks to one peak, i.e. $\lambda_1 =$ 728 nm, 668 nm, respectively) the position of the right side peak changes as the pump-1 laser intensity increases. There is a linear splitting proportional to $\sqrt{R_2^2 + \Delta_1^2}/2$ for the weak pump-1 field ($R_1 \ll R_2$), while the right side peak approaches to a linear splitting proportional to $R_1/2$ for the strong pump-1 field ($R_1 \gg R_2$).

References

[1] Autler S H and Townes C H 1955 *Phys. Rev.* **100** 703
[2] Wollenhaupt M, Assion A, Bazhan O, Horn Ch, Liese D, Sarpe-Tudoran Ch, Winter M and Baumert T 2003 *Phys. Rev. A* **68** 015401
[3] Wollenhaupt M, Liese D, Prakelt A, Sarpe-Tudoran C and Baumert T 2006 *Chem. Phys. Lett.* **419** 184
[4] Peng Y G and Zheng Y J 2008 *Appl. Phys. Lett.* **92** 092120
[5] Peng Y G and Zheng Y J 2009 *Phys. Rev. A* **80** 043831
[6] Sun Z G and Lou N Q 2003 *Phys. Rev. Lett.* **91** 023002

[7] Yuan K J, Sun Z G, Cong S L and Lou N Q 2006 *Phys. Rev. A* **74** 043421
[8] Liu Y F, Liu R Q and Ding J X 2009 *Chin. Phys. Lett.* **26** 073301
[9] Yao H B and Zheng Y J 2012 *Chin. Phys. B* **21** 023302
[10] Yao H B, Li W L, Zhang J and Peng M 2014 *Acta Phys. Sin.* **63** 178201 (in Chinese)
[11] Wei C J, Suter D, Windsor A S M and Manson N B 1998 *Phys. Rev. A* **58** 2310
[12] Han D A, Zeng Y G, Chen W C, Dong S G, Huang C Q, Zhu C Y and Liang P Y 2011 *Commun. Theor. Phys.* **55** 671
[13] Sadeghi S M, Meyer J and Rastegar H 1997 *Phys. Rev. A* **56** 3097
[14] Yang L J, Zhang L S, Zhuang Z H, Guo Q L and Fu G S 2008 *Chin. Phys. B* **17** 2147
[15] Yang L J, Zhang L S, Li X L, Han L, Fu G S, Manson N B, Suter D and Wei C J 2005 *Phys. Rev. A* **72** 053801
[16] Zhang L S, Li X L, Wang J, Yang L J, Feng X M, Li X W and Fu G S 2008 *Acta Phys. Sin.* **57** 4921 (in Chinese)
[17] de Echaniz S R, Greentree A D, Durrant A V, Segal D M, Marangos J P and Vaccaro J A 2001 *Phys. Rev. A* **64** 013812
[18] Wang D S and Zheng Y J 2011 *Phys. Rev. A* **83** 013810
[19] Dutta B K and Mahapatra P K 2009 *Phys. Scr.* **79** 065402
[20] Sandhya S N 2007 *J. Phys. B* **40** 837
[21] Haque I and Singh M R 2007 *J. Phys.* **19** 156229
[22] Meier C and Engel V 1994 *Phys. Rev. Lett.* **73** 3207
[23] Meier C, Engel V and Manthe U 1998 *J. Chem. Phys.* **109** 36
[24] Hu W H, Yuan K J, Han Y C, Shu C C and Cong S L 2007 *Chin. Phys. Lett.* **24** 1556
[25] Hu W H, Yuan K J, Han Y C, Shu C C and Cong S L 2010 *Inter. J. Quan. Chem.* **110** 1224
[26] Liu Y F, Liu R Q and Ding J X 2010 *Chin. Phys. B* **19** 033301
[27] Yao H B and Zheng Y J 2011 *Phys. Chem. Chem. Phys.* **13** 8900
[28] Zhang M, Tang T T and Zhang C M 2014 *Acta Phys. Sin.* **63** 023302 (in Chinese)
[29] Nicole C, Bouchene M A, Meier C, Magnier S, Schreiber E and Girard B 1999 *J. Chem. Phys.* **111** 7857
[30] Brixner T, Krampert G, Pfeifer T, Selle R and Gerber G 2004 *Phys. Rev. Lett.* **92** 208301
[31] Schlesinger M, Mudrich M, Stienkemeier F and Strunz W T 2010 *Chem. Phys. Lett.* **490** 245
[32] Magnier S and Millie Ph 1996 *Phys. Rev. A* **54** 204
[33] Magnier S, Aubert-Frecon M and Allouche A R 2004 *J. Chem. Phys.* **121** 1771
[34] Jtaij A, Allouche A R, Magnier S and Aubert-Frecon M 2008 *Can. J. Phys.* **86** 1409
[35] Jraij A, Allouche A R, Magnier S and Aubert-Frecon M 2009 *J. Chem. Phys.* **130** 244307
[36] Broyer M, Chevaleyre J, Delacretaz G, Martin S and Woste L 1983 *Chem. Phys. Lett.* **99** 206
[37] Jong G, Li L, Whang T J, Stwalley W C, Coxon J A, Li M and Lyyra A M 1992 *J. Mol. Spectrosc.* **155** 115
[38] Kowalczyck P, Kasahara S, Kabir Md H and Kato H 2003 *J. Mol. Spectrosc.* **220** 162
[39] Ilyabaev E and Kaldor U 1993 *J. Chem. Phys.* **98** 7126
[40] de Vivie-Riedle R, Kobe K, Manz J, Meyer W, Reischl B, Rutz S, Schreiber E and Woste L 1996 *J. Phys. Chem.* **100** 7789
[41] Zhang H, Han K L, Zhao Y, He G Z and Lou N Q 1997 *Chem. Phys. Lett.* **271** 204
[42] Xie T X, Zhao Y, Zhao M Y and Han K L 2003 *Phys. Chem. Chem. Phys.* **5** 2034
[43] Hu J, Han K L and He G Z 2005 *Phys. Rev. Lett.* **95** 123001
[44] Chu T S, Zhang Y and Han K L 2006 *Int. Rev. Phys. Chem.* **25** 201
[45] Du Z J, Zhang S G, Wu C J, Guan Y, Zhao W Y and Chang H 2010 *Chin. Phys. Lett.* **27** 104202
[46] Wilson E A, Manson N B, Wei C and Yang L J 2005 *Phys. Rev. A* **72** 063813
[47] Li X L, Liu H N and Yang Y 2011 *Acta Opt. Sin.* **31** 0102001
[48] Zhang H B, Khadka U, Song J P, Zhang Y P and Xiao M 2011 *EPL* **93** 23002
[49] Cardimona D A, Alsing P M, Mozer H and Rhodes C 2009 *Phys. Rev. A* **79** 063817
[50] Manka A S, Doss h M, Narducci L M and Ru P 1991 *Phys. Rev. A* **43** 3748
[51] Van Leeuwen M F, Parademetriou S and Stroud Jr C R 1996 *Phys. Rev. A* **53** 990
[52] Papademetriou S, Van Leeuwen M F and Stroud Jr C R 996 *Phys. Rev. A* **53** 997
[53] Chang R Y, Fang W C, He Z S, Ke B S, Chen P N and Tsai C C 2007 *Phys. Rev. A* **76** 053420
[54] Zhu S Y, Narducci L M and Scully M O 1995 *Phys. Rev. A* **52** 4791
[55] Singh M R 2008 *J. Phys. B* **41** 135401